

Polyethylenimine-coated polysulfone/bacterial biomass composite fiber as a biosorbent for the removal of anionic dyes: Optimization of manufacturing conditions using response surface methodology

Ha Neul Park*, Chul-Woong Cho**, Han Ah Choi***, and Sung Wook Won*,***,†

*Department of Ocean System Engineering, Gyeongsang National University,
38 Cheondaegukchi-gil, Tongyeong, Gyeongnam 53064, Korea

**School of Chemical Engineering, Chonbuk National University, Jeonju, Jeonbuk 54896, Korea

***Department of Marine Environmental Engineering and Institute of Marine Industry,
Gyeongsang National University, 38 Cheondaegukchi-gil, Tongyeong, Gyeongnam 53064, Korea

(Received 9 January 2017 • accepted 25 May 2017)

Abstract—This study aim was to optimize the manufacturing conditions polyethylenimine-coated polysulfone/bacterial biomass composite fiber (PEI-PSBF) to remove anionic pollutants from aqueous solution. The contents of biomass, PEI, and glutaraldehyde (GA) were selected as independent variables, and the response was defined as Reactive Yellow 2 (RY2) uptake. The manufacturing conditions were optimized by response surface methodology (RSM) with the full factorial central composite design (CCD). The determined coefficient of determination (R^2) value of the reduced quadratic model was 0.9551, and the optimal manufacturing conditions were predicted as 4.145 g of biomass, 1.104 g of PEI and 3.9 μ L of GA, at where the predicted RY2 uptake was 543.78 mg/g. For validating the RSM-predicted results, the RY2 sorption capacity of the optimized PEI-PSBF was evaluated through isotherm experiments. The experimentally confirmed maximal uptake was comparable to predicted one. From these studies, the manufacturing conditions for PEI-PSBF were well optimized and its sorption capacity was 3.83 times higher than that of the PSBF.

Keywords: Optimization, Response Surface Methodology, Central Composite Design, Adsorption, Reactive Dyes

INTRODUCTION

Dyes have been used for loose fiber dyeing, plastics, paper, and food additives. Dye-bearing wastewaters can be released into nature and exert adverse effects on the life cycle of living things in under-water environments [1]. Since even a low concentration of dye in wastewater results in thick colors, it can cause disagreeableness and negative aesthetic effects, leading to civil complaints [2]. Moreover, the released dyes also can block the sunlight passing through a water system; thus it can hinder the photosynthesis and growth of aquatic plants [3]. Although most dyes are known to be non-toxic, some can cause a carcinogenicity and mutation [4]. Therefore, it requires the appropriate treatment of dyes prior to the discharge into nature. The conventional methods for the removal of the synthetic dyes involve chemical, physical, and biological treatments; adsorption technology is especially known to be an economical and simple approach compared to the others [5,6].

Currently, the most popular adsorbent for dye adsorption is activated carbons, which boast high throughput efficiency, but their use is limited due to their expensive cost and difficult regeneration [7]. By contrast, biomass-based sorbents are very cheap and the exhausted ones can be easily regenerated. From the viewpoint of economical effectiveness, these facts make the biosorbent more prom-

ising [8,9].

Since *Escherichia coli* biomass has been massively cultivated by the fermentation industries for producing amino acids and the bacterial surface has many three functional groups such as carboxyl, phosphate and amine groups, it can be used as a promising raw material. These functional groups exhibit negative (carboxyl and phosphate groups) or positive (amine group) charges in aqueous solution at the different pH scales [10]. Indeed, *E. coli* biomass has been proven as a potential biosorbent for removing and/or recovering reactive dyes [11], ionic liquids [12], heavy metals [13], and precious metals [14] through the electrostatic interaction between the functional groups on the bacterial surface and target pollutants in solvent. However, the powder form of *E. coli* can make drains sluggish when it is applied to column systems in industries. Thus, the immobilization of the biomass has been tried to avoid the above problem.

Previously, polyvinyl alcohol immobilized recombinant *E. coli* and polysulfone-*E. coli* biomass composite fiber (PSBF) were developed and their sorption capacities were evaluated [15,16]. The immobilized biosorbents showed strong mechanical strength and acid resistance, whereas the sorption capacity was decreased compared to the raw biomass because the matrix of the composites reduced the functional groups to be able to bind target pollutants. In our previous paper [16], we introduced a new method for developing a powerful biosorbent, fabricated by combining PSBF with branched polyethylenimine (PEI), which contains a large amount of primary, secondary and tertiary amines. The PEI-coated PSBF (PEI-PSBF)

†To whom correspondence should be addressed.

E-mail: sungukw@gmail.com

Copyright by The Korean Institute of Chemical Engineers.

showed a significant improvement of sorption performance for platinum, palladium and ruthenium ions, respectively [16-18]. However, in spite of its remarkable sorption abilities for platinum group metals, the manufacturing process of the biosorbent has not been optimized yet. Moreover, the sorption performance of the PEI-PSBF for anionic dyes needs to be evaluated to extend the range of its application.

We therefore aimed to optimize the manufacturing conditions of the high-performance PEI-PSBF by using response surface methodology (RSM). RSM is a collection of mathematical and statistical techniques for designing experiments, building empirical model, and analyzing the effects of several major factors, and its objective is to simultaneously optimize the levels of independent variables to accomplish the best response [19,20]. In the present work, the RSM was successfully employed using the central composite design (CCD) to identify the various interactions of the independent variables affecting the dye sorbent capacity of the biosorbent. The optimal conditions for manufacturing the best PEI-PSBF were determined and demonstrated.

MATERIALS AND METHODS

1. Materials

The fermentation waste of *E. coli* biomass was dried by a spray-drying process for 24 h and supplied as a dried powder form from the fermentation industry (Daesang, Gunsan, Korea). Polysulfone (PS) and 99.8% of *N,N*-dimethylformamide (DMF) were purchased from Sigma-Aldrich Korea Ltd. (Yongin, Korea). Industrial grade PEI (MW: 70000, content: 50%) and 25 wt% GA were obtained from Habjung Moolsan Co., Ltd. (Seoul, Korea) and Junsei Chemical Co., Ltd. (Tokyo, Japan), respectively. As a model anionic reactive dye, Reactive Yellow 2 (RY2) was purchased from Sigma-Aldrich Korea Ltd.; its general characteristics are summarized in Table 1. All the other chemicals used in this work were of analytical grade.

2. Preparation of PEI-coated Polysulfone/Bacterial Biomass Composite Fibers

10% (w/v) of PS solution was prepared by mixing 10 g of PS with 100 mL of DMF solution for 10 h at 40 °C. A certain amount of *E. coli* biomass (1.455-4.145 g) was added into 20 mL of PS solution and then the mixture was sufficiently stirred at room temperature for 24 h. The well-mixed suspension was then extruded through a spinneret with 0.57 mm diameter into distilled water to make PSBF fibers. PSBF was several times washed with distilled water to get rid of impurities and then freeze-dried by a freeze dryer (TFD

Series, Ilshinbiobase, Korea). To modify the surface of the PSBF, 0.5 g of PSBF was mixed with 20 mL of PEI solution with different mass contents (0.391-2.409 g), which was adjusted and maintained at a desired pH value (pH 10.5) for 2 h at 25 °C. Subsequently, 25% of GA solution (3.9-24.1 µL) was added in drops to the mixture of PEI and PSBF for cross-linking between the amine groups in PEI molecules and anhydride groups in GA with stirring for additional 2 h. After the cross-linking reaction, the produced biosorbent, PEI-PSBF was washed several times with distilled water, lyophilized for more than two days and finally stored in a desiccator.

3. Biosorption Experiments

The biosorption of RY2 was conducted to estimate the sorption capacities of the biosorbents prepared at different manufacturing conditions. The experiments were carried out by mixing 30 mL of dye solution (500 mg/L) and 0.02 g of biosorbent in 50-mL polypropylene conical tubes. The solution was initially adjusted to pH 2 and kept during RY2 biosorption experiments using 1 M HCl or 1 M NaOH solution. The tubes were stirred at 160 rpm for 24 h at 25 °C. After the sorption equilibrium was reached, the final pH was measured by a pH meter (Orion Star A211, Thermo Fisher Scientific, USA) and centrifuged at 9,000 rpm for 5 min. The supernatant was taken and properly diluted with distilled water. Then, the residual dye concentration was analyzed at the maximum wavelength of RY2 (λ_{max} =404 nm) using a spectrophotometer (UVmini-1240, Shimadzu, Kyoto, Japan). The dye uptake (q (mg/g)) was finally calculated using the following mass balance equation:

$$q = \frac{C_i V_i - C_f V_f}{m} \quad (1)$$

where C_i and C_f are the initial and final dye concentrations (mg/g), respectively; V_i and V_f mean the initial and final solution volumes (L), respectively; m is the mass of biosorbent (g).

To confirm the maximum sorption capacity of the optimized biosorbent, the biosorption isotherms were additionally evaluated at pH 2. The initial RY2 concentrations were in the range of 0-1,000 mg/L, which led to different final dye concentrations in a state of equilibrium. The remaining procedures were the same as in the above sorption experiments.

4. Experimental Design for the Optimization of PEI-PSBF Manufacturing Conditions

An experimental design technique is useful for finding the optimized condition of some major factors, to improve the performance, and to minimize the error of experiments [21]. In this study, the CCD with the two-level full factorial design for three factors was

Table 1. General characteristics of Reactive Yellow 2

| | | |
|----------------------|------------------------------------|---------------------|
| Color index | 18972 | Molecular structure |
| Molecular formula | $C_{25}H_{15}Cl_3N_9Na_3O_{10}S_3$ | |
| Molecular weight | 872.97 | |
| Dye content (%) | 60-70 | |
| λ_{max} (nm) | 404 | |

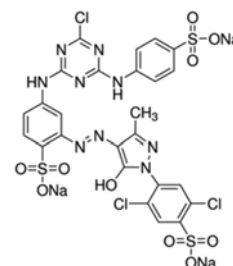


Table 2. Levels of the independent variables in the central composite design

| Independent variable | Symbol | Level | | | | |
|----------------------|--------|--------|-----|-----|-----|--------|
| | | -1.682 | -1 | 0 | +1 | +1.682 |
| Biomass (g) | X_1 | 1.455 | 2 | 2.8 | 3.6 | 4.145 |
| PEI (g) | X_2 | 0.391 | 0.8 | 1.4 | 2.0 | 2.409 |
| GA (μ L) | X_3 | 3.9 | 8 | 14 | 20 | 24.1 |

combined with the RSM to find the optimal manufacturing conditions of PEI-PSBF. Based on the preliminary experiments, the contents of the biomass, PEI, and GA were selected as independent variables and coded as X_1 , X_2 , and X_3 , respectively. The response (Y) was defined as the RY2 uptake and depended on the independent variables. Each independent variable was encoded into five different levels (-1.682, -1, 0, +1, +1.682) as given in Table 2. From the CCD model, the number of experimental runs was calculated using the following equation:

$$N = 2^k + 2k + x_0 \quad (2)$$

where N is the number of experimental runs, k is the number of factors, and x_0 is the number of central points [22]. Since the number of k and x_0 was both 3, the total experimental runs were calculated to be 17. A total of 17 experimental runs including eight factorial, six star, and three central points were designed and analyzed by Design Expert 9.0.6 software (Stat-Ease Inc., Minneapolis, USA).

The mathematical relationship between the response (dependent variable) and the three independent variables can be expressed by the second-order polynomial model as follows:

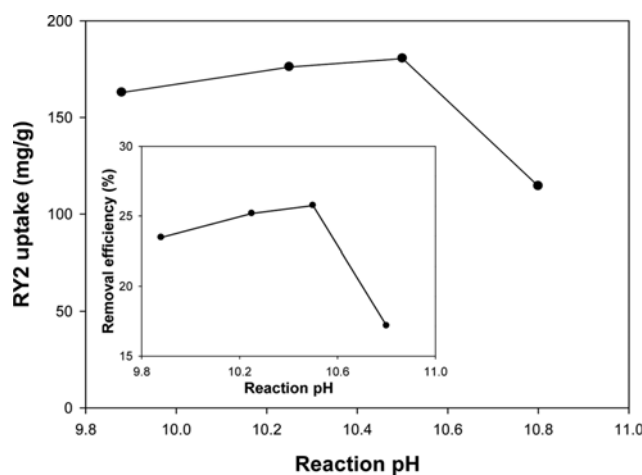
$$Y = \beta_0 + \sum_{i=1}^k \beta_i X_i + \sum_{i=1}^k \beta_{ii} X_i^2 + \sum_{i=1}^{k-1} \sum_{j=2}^k \beta_{ij} X_i X_j + \varepsilon \quad (3)$$

where Y is the predicted response (RY2 uptake). X_i and X_j are the independent variables in coded levels. β_0 , β_i , and β_{ij} are the coefficients for linear, quadratic and interaction effects, respectively. β_0 is the model coefficient, k is the number of factors (independent variables), and ε is a random error [23]. The least square method was used to calculate the model coefficients through Eq. (3) using Design Expert 9.0.6 software. To evaluate the statistical significance, analysis of variance (ANOVA), normal plots and residuals analyses were employed. The significance of the regression coefficients was appraised by the P - and F -values at the confidence level of 95%.

RESULTS AND DISCUSSION

1. Effect of Reaction pH

Our previous study [16] reported that PEI-PSBF can be manufactured by a three-step procedure: first, to prepare the PSBF, second, to induce the electrostatic binding between the PEI (positively charged amine groups) and *E. coli* biomass (negatively charged functional groups), and third, to chemically bond PEI polymer using a cross-linker to enhance durability of the sorbent. Among these steps, the amount of PEI introduced in the PSBF can be decided

**Fig. 1. Effect of reaction pH on the RY2 sorption capacity of PEI-PSBF.**

through the second step. In this step, pH scale on the reaction plays a vital role in the binding between the PEI molecules and *E. coli* biomass because it can electrostatically affect the strength or ionization of functional groups [24]. Therefore, to maximize the sorption capacity of RY2 onto the PEI-PSBF, we needed to identify the optimal reaction pH in biosorbent manufacturing processes.

The pK_a value of the amine groups on the surface of *E. coli* biomass is in the range of 8-9 [10]. On the other hand, the pK_a values of PEI are 4.5, 6.7, and 11.6 for the primary, secondary, and tertiary amine groups, respectively [25]. To minimize the interference between the amine groups in *E. coli* and PEI, the reaction pH was selected to be 9.8-10.8. Therefore, four different PEI-PSBFs fabricated in the selected pH range were prepared and their sorption capacities for RY2 were also evaluated to find an optimal reaction pH for manufacturing a high-sorption biosorbent. Their sorption capacities were estimated at 500 mg/L of dye concentration for 24 h at 25 °C. The results are expressed in Fig. 1. The sorption capacity increased from 162.9 to 180.5 mg/g as increasing the reaction pH from 9.88 to 10.5. On the other hand, the sorption capacity of the PEI-PSBF prepared at reaction pH 10.8 was significantly decreased to 114.5 mg/g. This phenomenon may be explained as the interaction effects related to the specific functional groups between the PEI and biomass exposed on the surface of PSBF. As a result, the reaction pH was evaluated as an important factor in development of powerful biosorbents and pH 10.5 was decided to be the optimal reaction pH when the PEI molecules were coated on the surface of PSBF.

2. Analysis of Central Composite Design

To investigate the optimal fabrication conditions of the PEI-PSBF with high-capacity, the dosages of the biomass (X_1), PEI (X_2) and GA (X_3) were selected as independent variables into five levels as coded values (-1.682, -1, 0, +1, +1.682). As presented in Table 3, 17 manufacturing conditions were designed by the CCD, and their biosorbents were then prepared in a random order to minimize the effect of uncontrolled factors. As the responses of all designed experiments, RY2 uptakes were achieved through batch sorption experiments at pH 2. The experimental and predicted

Table 3. The 3-factor central composite design matrix and the values of the actual and predicted RY2 uptakes

| Run | Independent variable | | | | | | Response | |
|-----|----------------------|----------------|----------------|-------------|---------|---------|-------------------|-------------------|
| | Coded value | | | Real value | | | RY2 uptake (mg/g) | |
| | X ₁ | X ₂ | X ₃ | Biomass (g) | PEI (g) | GA (μL) | q _{exp} | q _{pred} |
| 1 | −1 | −1 | −1 | 2 | 0.8 | 8 | 180.48 | 180.78 |
| 2 | +1 | −1 | −1 | 3.6 | 0.8 | 8 | 374.11 | 369.50 |
| 3 | −1 | +1 | −1 | 2 | 2 | 8 | 250.89 | 252.46 |
| 4 | +1 | +1 | −1 | 3.6 | 2 | 8 | 352.10 | 370.77 |
| 5 | −1 | −1 | +1 | 2 | 0.8 | 20 | 237.69 | 233.36 |
| 6 | +1 | −1 | +1 | 3.6 | 0.8 | 20 | 242.09 | 254.85 |
| 7 | −1 | +1 | +1 | 2 | 2 | 20 | 299.30 | 305.03 |
| 8 | +1 | +1 | +1 | 3.6 | 2 | 20 | 255.29 | 256.12 |
| 9 | −1.682 | 0 | 0 | 1.455 | 1.4 | 14 | 277.29 | 279.07 |
| 10 | +1.682 | 0 | 0 | 4.145 | 1.4 | 14 | 409.31 | 396.59 |
| 11 | 0 | −1.682 | 0 | 2.8 | 0.391 | 14 | 198.08 | 199.35 |
| 12 | 0 | +1.682 | 0 | 2.8 | 2.409 | 14 | 272.89 | 260.68 |
| 13 | 0 | 0 | −1.682 | 2.8 | 1.4 | 3.9 | 312.50 | 289.29 |
| 14 | 0 | 0 | +1.682 | 2.8 | 1.4 | 24.1 | 259.69 | 237.04 |
| 15 | 0 | 0 | 0 | 2.8 | 1.4 | 14 | 246.49 | 263.16 |
| 16 | 0 | 0 | 0 | 2.8 | 1.4 | 14 | 259.69 | 263.16 |
| 17 | 0 | 0 | 0 | 2.8 | 1.4 | 14 | 246.49 | 263.16 |

Table 4. ANOVA for quadratic model parameters

| Source | Full quadratic model | | | | | Reduced quadratic model | | | | |
|-------------------------------|-----------------------------|----|----------------------------|------------|---------|-----------------------------|----|----------------------------|------------|---------|
| | Sum of squares | DF | Mean square | F-value | Prob>F | Sum of squares | DF | Mean square | F-value | Prob>F |
| Model | 54634.67 | 9 | 6070.52 | 27.10 | 0.0001 | 53679.89 | 7 | 7668.56 | 27.36 | <0.0001 |
| X ₁ | 16678.06 | 1 | 16678.06 | 74.45 | <0.0001 | 16678.06 | 1 | 16678.06 | 59.50 | <0.0001 |
| X ₂ | 4540.76 | 1 | 4540.76 | 20.27 | 0.0028 | 4540.76 | 1 | 4540.76 | 16.20 | 0.0030 |
| X ₃ | 3291.77 | 1 | 3291.77 | 14.69 | 0.0064 | 3291.77 | 1 | 3291.77 | 11.74 | 0.0075 |
| X ₁ X ₂ | 2479.14 | 1 | 2479.14 | 11.07 | 0.0126 | 2479.14 | 1 | 2479.14 | 8.84 | 0.0156 |
| X ₁ X ₃ | 13982.10 | 1 | 13982.10 | 62.41 | <0.0001 | 13982.10 | 1 | 13982.10 | 49.88 | <0.0001 |
| X ₂ X ₃ | 87.19 | 1 | 87.19 | 0.39 | 0.5525 | - | - | - | - | - |
| X ₁ ² | 9476.73 | 1 | 9476.73 | 42.30 | 0.0003 | 8609.63 | 1 | 8609.63 | 30.71 | 0.0004 |
| X ₂ ² | 938.43 | 1 | 938.43 | 4.19 | 0.0799 | 1696.20 | 1 | 1696.20 | 6.05 | 0.0362 |
| X ₃ ² | 867.59 | 1 | 867.59 | 3.87 | 0.0898 | - | - | - | - | - |
| Residual | 1568.15 | 7 | 224.02 | | | 2522.93 | 9 | 280.33 | | |
| Lack of fit | 1451.99 | 5 | 290.40 | 5.00 | 0.1750 | 2406.77 | 7 | 343.82 | 5.92 | 0.1521 |
| Pure error | 116.16 | 2 | 58.08 | | | 116.16 | 2 | 58.08 | | |
| Total | 56202.82 | 16 | | | | 56202.82 | 16 | | | |
| | R ² =0.9721 | | Adj R ² =0.9362 | C.V.%=5.44 | | R ² =0.9551 | | Adj R ² =0.9202 | C.V.%=6.09 | |
| | Pred R ² =0.7931 | | Adeq precision=17.936 | | | Pred R ² =0.8517 | | Adeq precision=18.790 | | |

values are given in Table 3. The actual values well agreed on the predicted ones. Also, the main, interactive, and quadratic effects of three major factors on RY2 sorption were estimated in this design.

The mathematical relationship between the coded independent variables and response was drawn by the second-order polynomial model, and the best fitted equation was obtained as follows:

$$Y = 251.95 + 34.95X_1 + 18.23X_2 - 15.52X_3 - 17.60X_1X_2 - 41.81X_1X_3 + 3.30X_2X_3 + 29.01X_1^2 - 9.13X_2^2 + 8.76X_3^2 \quad (4)$$

In this equation, the plus and minus signs of the determined coefficients represent the synergistic and antagonistic effects, respectively [26]. ANOVA has been often used to estimate the significance of the main, interactive, and quadratic effects of independent variables. As presented in Table 4, the ANOVA table was obtained from Design Expert 9.0.6 software, and the statistical signification of the model used in the present study was checked by ANOVA. In the ANOVA table, the *P*-value (*P*<0.05) and the large *F*-value mean the significance of independent variables at 95% confidence

level [27]. The P - and F -values of the model were estimated to be 0.0001 and 27.10, respectively. Also, the determination coefficient (R^2) value was 0.9721. It shows that the second-order polynomial model is statistically significant and the selected independent variables have a substantial force on various responses. In conditions of code factors, the linear (X_1 , X_2 , X_3), quadratic (X_1^2), and cross-product (X_1X_2 , X_1X_3) terms were statistically significant because their P -values were lower than 0.05, while the quadratic terms of X_2^2 and X_3^2 and cross-product term of X_1X_3 were not important because of their large P -values (>0.05). Therefore, these insignificant model terms need to be eliminated to enhance the degree of adequacy and tolerability of the model. For this, they were taken out from the response surface quadratic model by using a backward elimination method, and the new ANOVA table for the response surface reduced quadratic model was derived and given in Table 4, and the final model could be expressed as the following equation:

$$Y = 263.16 + 34.95X_1 + 18.23X_2 - 15.52X_3 - 17.60X_1X_2 - 42.81X_1X_3 + 26.42X_1^2 - 11.72X_2^2 \quad (5)$$

The model parameters of F -value, predicted R^2 , and adequate precision were improved from 27.10, 0.7931 and 17.936 to 27.36,

0.8517 and 18.790, respectively. As seen in Table 4, the reduced quadratic model was statistically acceptable due to the F -value of 27.36 and low P -value (<0.0001) of the used parameters. Again, the F -value of the model was larger than the critical F -value ($F_{0.05,7,9} = 3.29$), suggesting that the computed Fisher's Variance ratio at this level was extremely enough to confirm the adequacy of the reduced quadratic model [28]. In addition, the R^2 value of 0.9551 also implied that the reduced quadratic model could offer a good correlation between the independent variables and responses. The F -value of lack of fit was 5.92, which suggested that lack of fit was not significant regarding the pure error and insignificance of lack of fit confirmed good model efficiency for the prediction of the RY2 uptake by biosorbents used in this work. The entire main (X_1 , X_2 , X_3), interactive (X_1X_2 , X_1X_3), and quadratic (X_1^2 , X_2^2) effects were found to be statistically significant as their P -values were lower than 0.05. The predicted R^2 of 0.8517 was in reasonable agreement with the adjusted R^2 of 0.9202, since the difference between them was less than 0.2 [29]. Adequate precision measures the signal-to-noise ratio for the uptake of RY2, and a ratio greater than 4 is desirable [30]. In this sense, the ratio of 18.790 indicates an adequate signal. Finally, the relatively low coefficient of variation (C.V.) of 6.09%

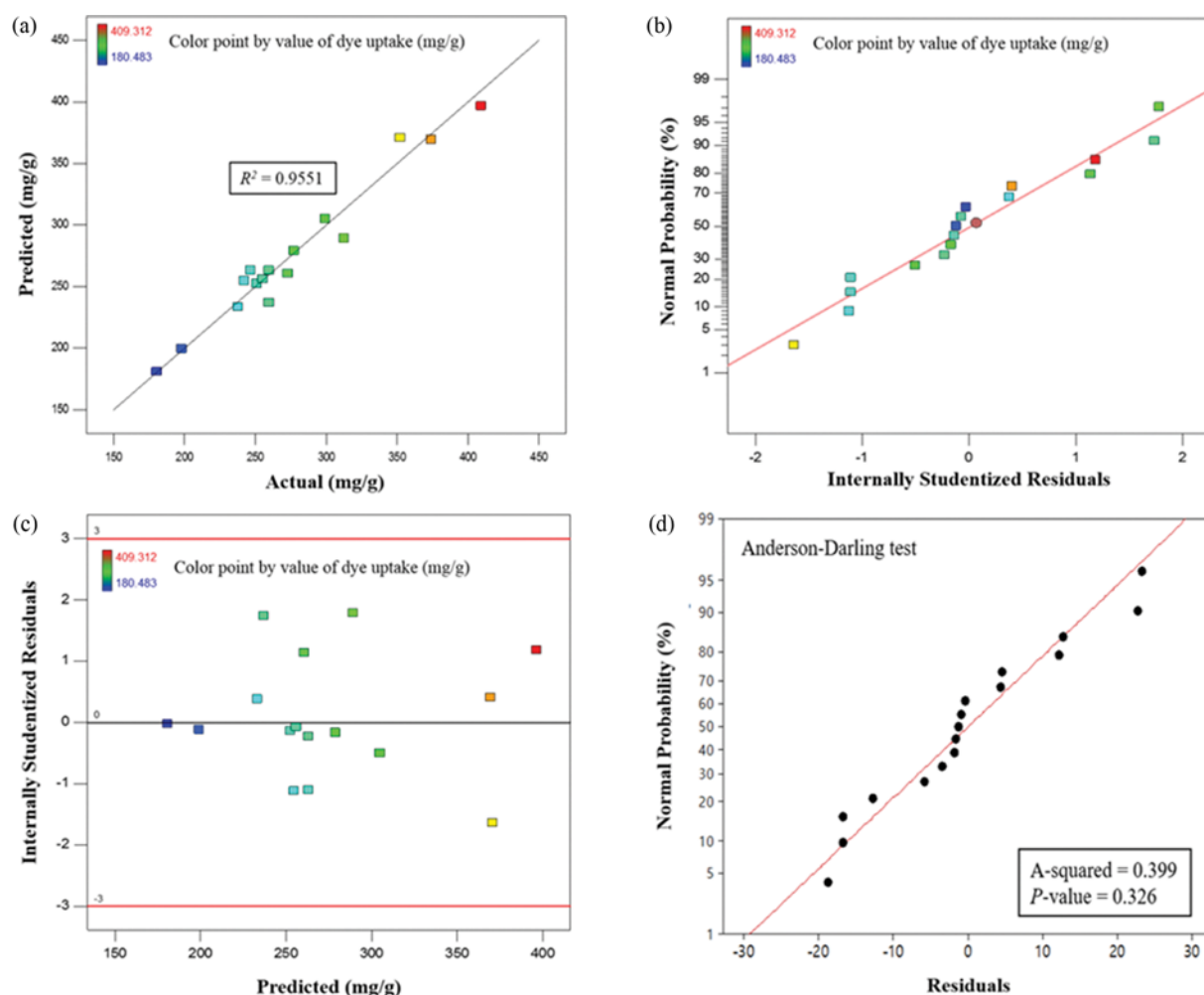


Fig. 2. (a) A plot of the actual and predicted RY2 uptake values, (b) the normal probability of the residuals, (c) the scatter diagram of residuals and predicted, and (d) the Anderson-Darling test and normal probability plots.

indicates the good reliability of the model. These values, discussed above, confirm high acceptability of the reduced quadratic model for the best predicting the RY2 uptake of the PEI-PSBF.

The comparison of experimental and predicted RY2 uptake is depicted in Fig. 2(a). Fig. 2(a) shows a good agreement between the predicted and experimental RY2 uptake. The obtained R^2 value of 0.9551 shows that 95.51% of the variations for the RY2 uptake (mg/g) can be accounted for by the model, while the rest of the variations (4.49%) are not explainable. In addition, the adequacy of the model can be identified through the evaluation of the residuals calculated by determining the difference between the experimental and predicted RY2 uptake [31]. The normal probability graph of residuals was plotted for RY2 uptake and given in Fig. 2(b). As shown in Fig. 2(b), the data points appeared on a straight line and the residuals were normally distributed. Furthermore, Fig. 2(c) shows the scatter plot of the predicted versus residuals values. The residuals in the plot were randomly distributed around the center, meeting the homoscedasticity of the errors. The Anderson-Darling test in order to examine the normal probability plot of the residuals for the dependent variable (RY2 uptake) is shown in Fig. 2(d). As a result, the data almost followed a straight line and the P -value was greater than 0.05, which means that the proposed model is adequate. Therefore, the reduced quadratic model as Eq. (5) can be applied to predict the uptake of RY2 by the PEI-PSBF in the limited range of the selected independent variables with reasonably good accuracy.

3. Determination of Optimal Conditions

Response surface and contour plots are generally used to determine various interactions of any two variables. These are useful in understanding of the main effects as well as the interaction effects between two factors. The response surface and contour plots for the measured responses were drawn as Figs. 3 and 4 based on the reduced quadratic model Eq. (5).

Fig. 3(a) and (b) show the 3D response surface and contour plots as a function of the dosages of biomass (X_1) and GA (X_3) at the center level of the PEI (X_2). As the content of the *E. coli* biomass contained in the PSBF was increased, the RY2 uptake rapidly increased (Fig. 3(a)). Also, a desirable biomass dosage for

maximizing the RY2 sorption capacity was around 4.145 g in the studied range, while the GA dosage should be decreased when the biomass dosage is increased. In the case of GA dosage, increasing the content of GA resulted in the increase of the RY2 uptake at $-\alpha$ level (1.455 g) of the biomass. As seen in Fig. 3(b), the uptake of RY2 reached above 500 mg/g at the conditions of 3.9 μ L of GA and 4.145 g of biomass. These phenomena could be explained based on the roles of the biomass and GA in the PEI-PSBF. In detail, the biomass exposed on the surface of the PSBF provides specific binding sites, such as negatively charged carboxyl groups, to combine the positively charged amine groups in PEI molecules [32]. Thus, an increase of biomass content leads to increase the quantity of PEI on the PSBF surface. On the contrary, the main role of GA is to reinforce mechanical strength of the biosorbent by cross-linking the amine groups in PEI molecules with its anhydride groups. However, an increase of its amount can reduce the amine groups in PEI for RY2 biosorption [19,33]. Thus, the dosage of GA needs to be minimized to maximize the dye sorption capacity of sorbent.

Fig. 4(a) and (b) present the 3D response surface and contour plots between the biomass (X_1) and PEI (X_2) dosages on the RY2 uptake at the $-\alpha$ level of GA (X_3). It was clearly shown that the RY2 uptake was depending on the variables, i.e., quantities of biomass and PEI. The RY2 uptake of the PEI-PSBF remarkably increased as the biomass dosage was increased from 1.455 to 4.145 g, and also the increase of PEI dosage from 0.391 to 2.409 g led to a slight enhancement of RY2 sorption capacity, as shown in Fig. 4(a). In the case of the contour plot (Fig. 4(b)), the PEI-PSBF showed the 543 mg/g of RY2 uptake at 4.145 g of biomass and 1.1 g of PEI. More addition of PEI up to 1.4 g resulted in a slight increase of RY2 uptake. However, further addition of PEI over 1.4 g rather tended to decrease the RY2 uptake of the PEI-PSBF. From these findings, it can be concluded that greater amount of biomass provides more functional groups so that PEI molecules can be much bound on the surface of the biosorbent, and excess PEI amount does not help to enhance the sorption capacity for RY2.

The numerical optimization for the PEI-PSBF manufacturing conditions using Design Expert 9.0.6 software was estimated. Here,

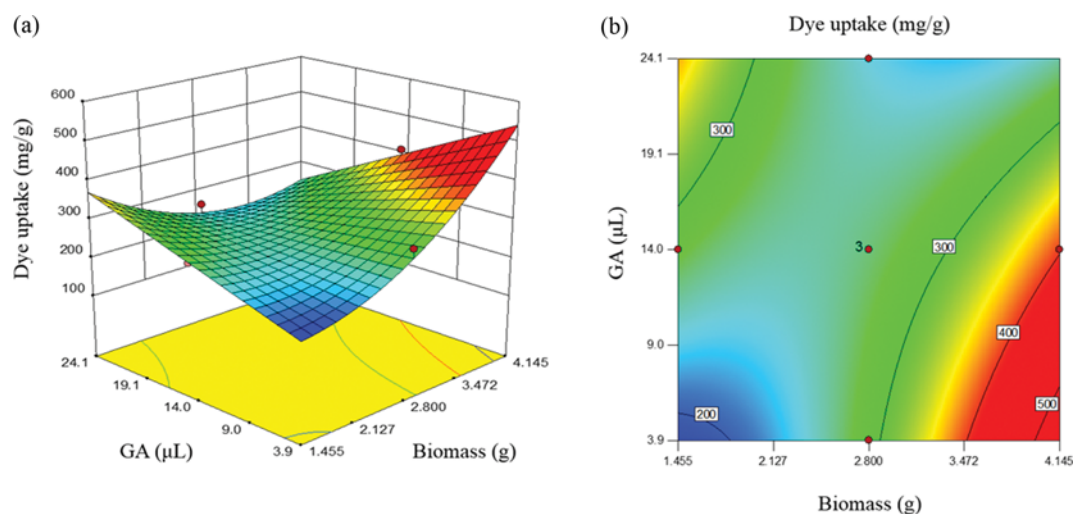


Fig. 3. (a) 3D response surface plot and (b) corresponding contour plot of the RY2 uptake as the function of GA and biomass dosages.

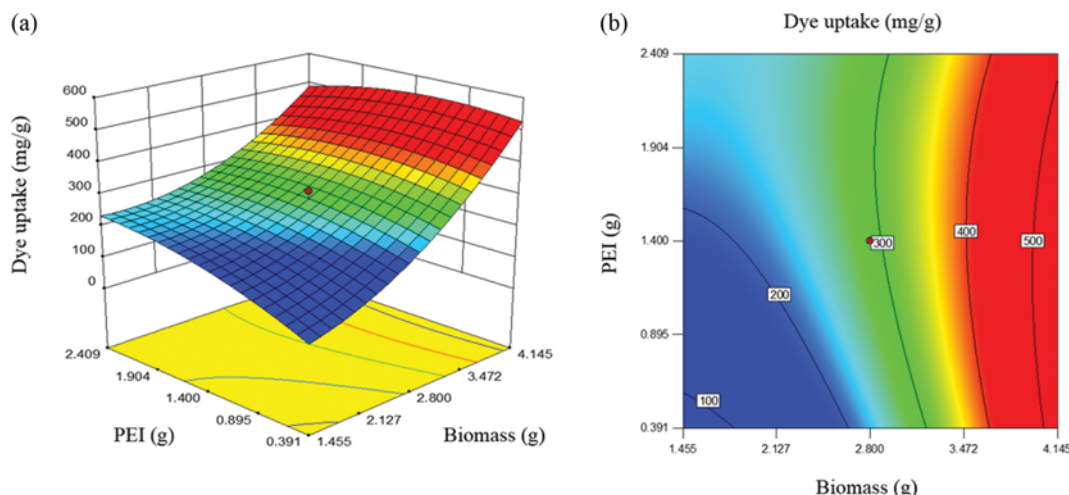


Fig. 4. (a) 3D response surface plot and (b) corresponding contour plot of the RY2 uptake as the function of PEI and biomass dosages.

Table 5. Optimum values of the variables and response

| Variable | Symbol | Optimum value | Response | Symbol | Optimum value |
|---------------|--------|---------------|-------------------|--------|---------------|
| Biomass (g) | X_1 | 4.145 | RY2 uptake (mg/g) | Y | 543.78 |
| PEI (g) | X_2 | 1.104 | | | |
| GA (μ L) | X_3 | 3.9 | | | |

the desirability function was maximized at the biomass dosage in range of 1.455–4.145 g, PEI dosage in the range of 0.391–2.409 g, GA volume in the range of 3.9–24.1 μ L, and maximum level for RY2 uptake. As a result, the local maximum was found at 4.145 g of biomass, 1.104 g of PEI, and 3.9 μ L of GA as given in Table 5. In these conditions, the RY2 uptake was predicted to be 543.72 mg/g at pH 2 and the initial RY2 concentration of 500 mg/L.

4. Confirmation of the RSM Validity through Biosorption Isotherms

To confirm the RSM validity, the PEI-PSBF was prepared at the optimal manufacturing conditions of 4.145 g of biomass, 1.104 g of PEI and 3.9 μ L of GA. The RY2 sorption capacity of the optimized PEI-PSBF was evaluated to be 540.52 mg/g at pH 2 and 500 mg/L of the initial dye concentration, which was comparable to the predicted q value (543.78 mg/g) by RSM. It indicates that the theoretical optimization for PEI-PSBF manufacturing conditions has been successfully performed.

The biosorption isotherms of the PSBF and PEI-PSBF were carried out at pH 2 by varying the initial RY2 concentration within the range of 0–1,000 mg/L, with a constant biosorbent dosage of 0.02 g. As shown in Fig. 5, the RY2 uptakes of the PSBF and PEI-PSBF were sharply increased at lower dye concentrations, while the isotherm shapes were concave curves with a strict plateau. Modeling of the RY2 isotherm data was attempted using the non-linear form of the Langmuir model as the following equation:

$$q = \frac{q_{\max} b C_f}{1 + b C_f} \quad (6)$$

where C_f is the final dye concentration (mg/L), q_{\max} is the maximum dye uptake (mg/g), and b is the Langmuir equilibrium con-

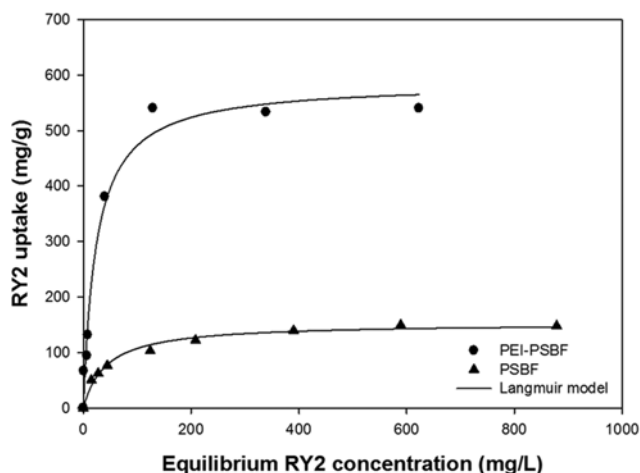


Fig. 5. Biosorption isotherms for the RY2 sorption capacities of the PSBF and optimized PEI-PSBF. Isotherm experiments were carried out at pH 2 and the isotherm experimental data were fitted by the Langmuir model (solid lines).

stant (L/mg) related to the affinity between the sorbate and sorbent. The Langmuir parameters and coefficients of determination are summarized in Table 6. The Langmuir model incorporates two easily interpretable constants: q_{\max} , which is often used to compare the performance of biosorbents; and b , which relates to the affinity between the sorbate and sorbent. Hence, for a good biosorbent, a high q_{\max} and a high b (i.e., steep initial isotherm slope) are desirable [34]. For both isotherm curves by Langmuir model were fitted within the R^2 value of 0.982. According to the Langmuir

Table 6. Langmuir parameters for RY 2 biosorption by the PSBF and optimized PEI-PSBF at pH 2

| Biosorbent | Langmuir model ^a | | |
|------------|-----------------------------|-----------------|----------------|
| | q _{max} (mg/g) | b (L/mg) | R ² |
| PSBF | 153.24 (4.70) | 0.0234 (0.0031) | 0.9847 |
| PEI-PSBF | 586.76 (26.24) | 0.0415 (0.0085) | 0.9822 |

^aStandard errors are in parentheses

model, the maximum sorption capacities were found to be 153.24 and 586.76 mg/g for the PSBF and PEI-PSBF, respectively. This suggests that the PEI-PSBF was successfully fabricated at the optimal manufacturing conditions and a large amount of amine groups were included in the PEI-PSBF, which resulted in the 3.83 times enhancement of sorption capacity compared to that of the PSBF. Moreover, the values of affinity (b) showed 0.0234 and 0.0415 L/mg for the PSBF and PEI-PSBF, respectively. The higher b value for the PEI-PSBF may be attributed to the fact that the binding sites for RY2 sorption mainly exist on the surface of the PEI-PSBF.

CONCLUSIONS

The aim was to optimize the manufacturing processes for a high-capacity PEI-PSBF, which has the maximum RY2 uptake, using the CCD and RSM. Before the optimization, pH 10.5 was selected as the optimum reaction pH based on our preliminary experiment. The optimal manufacturing conditions of PEI-PSBF were 4.145 g of *E. coli* biomass, 1.104 g of PEI, and 3.9 µL of GA at pH 10.5. The RY2 uptake of the optimized PEI-PSBF was estimated to be 540.52 mg/g, almost the same as RSM predicted (543.78 mg/g). From the isotherm studies, the maximum sorption capacity of PEI-PSBF produced under the optimized manufacturing conditions was 3.83-fold higher than that of PSBF for RY2 biosorption. In conclusion, RSM can be effectively used to find the manufacturing conditions and the PEI-PSBF produced at the optimized conditions may be expected to be used for the removal of anionic dyes from aqueous solutions if its application studies are further investigated.

ACKNOWLEDGEMENTS

This work was supported by Basic Science Research Program through the National Research Foundation of Korea (NRF) funded by the Ministry of Science, ICT & Future Planning (NRF-2017R1A1A1A05000741), and partially supported by the Brain Korea 21 plus project.

REFERENCES

1. G. Bayramoğlu, G. Çelik and M. Y. Arica, *J. Hazard. Mater.*, **137**, 1689 (2006).
2. M. K. Purkait, S. DasGupta and S. De, *J. Environ. Manage.*, **76**, 135 (2005).

3. M. Punzi, F. Nilsson, A. Anbalagan, B.-M. Svensson, K. Jönsson, B. Mattiasson and M. Jonstrup, *J. Hazard. Mater.*, **292**, 52 (2015).
4. Z. Aksu, *Process Biochem.*, **40**, 997 (2005).
5. G. Z. Kyzas, J. Fu and K. A. Matis, *Materials*, **6**, 5131 (2013).
6. G. Crini, *Bioresour. Technol.*, **97**, 1061 (2006).
7. J. Gao, Q. Zhang, K. Su, R. Chen and Y. Peng, *J. Hazard. Mater.*, **174**, 215 (2010).
8. J. Wang and C. Chen, *Biotechnol. Adv.*, **27**, 195 (2009).
9. I. Michalak, K. Chojnacka and A. Witek-Krowiak, *Appl. Biochem. Biotechnol.*, **170**, 1389 (2013).
10. K. Vijayaraghavan and Y.-S. Yun, *Biotechnol. Adv.*, **26**, 266 (2008).
11. S. Kim, S. W. Won, C.-W. Cho and Y.-S. Yun, *Desalin. Water Treat.*, **57**, 20084 (2015).
12. S. W. Won, S. B. Choi, J. Mao and Y.-S. Yun, *J. Hazard. Mater.*, **244-245**, 130 (2013).
13. I. S. Kwak, S. W. Won, S. B. Choi, J. Mao, S. Kim, B. W. Chung and Y.-S. Yun, *Korean J. Chem. Eng.*, **28**, 927 (2011).
14. S. Kim, M.-H. Song, W. Wei and Y.-S. Yun, *J. Hazard. Mater.*, **283**, 657 (2015).
15. W.-C. Kao, J.-Y. Wu, C.-C. Chang and J.-S. Chang, *J. Hazard. Mater.*, **169**, 651 (2009).
16. S. W. Won, S. Kim, P. Kotte, A. Lim and Y.-S. Yun, *J. Hazard. Mater.*, **263**, 391 (2013).
17. C.-W. Cho, S. B. Kang, S. Kim, Y.-S. Yun and S. W. Won, *Chem. Eng. J.*, **302**, 545 (2016).
18. S. Kim, Y.-E. Choi and Y.-S. Yun, *J. Hazard. Mater.*, **313**, 29 (2016).
19. J. Mao, I.-S. Kwak, M. Sathishkumar, K. Sneha and Y.-S. Yun, *Bioresour. Technol.*, **102**, 1462 (2011).
20. M. A. Bezerra, R. E. Santelli, E. P. Oliveira, L. S. Villar and L. A. Escalera, *Talanta*, **76**, 965 (2008).
21. M. Kolaei, K. Dashtian, Z. Rafiee and M. Ghaedi, *Ultrason. Sonochem.*, **33**, 240 (2016).
22. A. Hassani, A. Khataee, S. Karaca, M. Karaca and M. Kırışan, *J. Environ. Chem. Eng.*, **3**, 2738 (2015).
23. A. Özer, G. Gürbüz, A. Çalimli and B. K. Körbahti, *Chem. Eng. J.*, **146**, 377 (2009).
24. S. Kim, D. H. K. Reddy, Y.-E. Choi and Y.-S. Yun, *J. Taiwan Inst. Chem. Eng.*, **66**, 379 (2016).
25. K. D. Demadis, M. Paspalaki and J. Theodorou, *Ind. Eng. Chem. Res.*, **50**, 5873 (2011).
26. M. Abbasi and M. M. Habibi, *J. Taiwan Inst. Chem. Eng.*, **62**, 112 (2016).
27. H. Sohbatazadeh, A. R. Keshtkar, J. Safdari and F. Fatemi, *Int. J. Biol. Macromol.*, **89**, 647 (2016).
28. K. P. Singh, A. K. Singh, S. Gupta and S. Sinha, *Desalination*, **270**, 275 (2011).
29. S. Chamoli, *Alexandria Eng. J.*, **54**, 429 (2015).
30. Y. Ding and M. Sartaj, *J. Environ. Chem. Eng.*, **3**, 807 (2015).
31. R. Darvishi Cheshmeh Soltani, A. Rezaee, A. R. Khataee and M. Safari, *J. Ind. Eng. Chem.*, **20**, 1861 (2014).
32. S. W. Won, I. S. Kwak and Y.-S. Yun, *Bioresour. Technol.*, **160**, 93 (2014).
33. S. Deng and Y.-P. Ting, *Water Res.*, **39**, 2167 (2005).
34. D. Kratochvil and B. Volesky, *Trends Biotechnol.*, **16**, 291 (1998).